

# TERMITES DETECTION VIA SPECTRAL KURTOSIS AND WAVELET DE-NOISING OF ACOUSTIC EMISSION SIGNALS

JUAN-JOSÉ G. DE LA ROSA<sup>1</sup>, ANTOLINO GALLEGO<sup>2</sup>, ROSA PIOTRKOWSKI<sup>3</sup>,  
ENRIQUE CASTRO<sup>2</sup> and ANTONIO MORENO-MUÑOZ<sup>4</sup>

<sup>1</sup>University of Cádiz, Electronics Area, Research Group PAIDI-TIC-168. Algeciras Polytechnic School, 11202 Algeciras-Cádiz, Spain; <sup>2</sup>Univ. of Granada, Dept. of Applied Physics, 18071 Granada, Spain; <sup>3</sup>Escuela de Ciencia y Tecnología, Universidad Nacional San Martín, Buenos Aires, Argentina, <sup>4</sup>University of Córdoba, Electronics Area, Research Group PAIDI-TIC-168. Campus Rabanales. Edificio Albert Einstein, 14071 Córdoba, Spain

**Keywords:** Higher-Order Statistics, Insect detection, Spectral Kurtosis.

## Abstract

In this paper we present the operation results of a portable computer-based measurement equipment conceived to perform non-destructive testing of suspicious termite infestations. Its signal processing module is based in the Spectral Kurtosis (SK), with the de-noising complement of the discrete wavelet transform (DWT). The SK pattern allows the targeting of alarms and activity signals. The DWT complements the SK, by keeping the successive approximations of the termite emissions, supposed more non-Gaussian (less noisy) and with less entropy than the detail approximations. For a given mother wavelet, the maximum acceptable level, in the wavelet decomposition tree, which preserves the insects' emissions features, depends on the comparative evolution of the approximations details' entropies, and the value of the global spectral kurtosis associated to the approximation of the separated signals. The paper explains the detection criterion by showing different types of real-life recordings (alarms, activity, and background).

## Introduction

Biological transients gather all the natural complexity of their associated sources, and the media through which they propagate. As a consequence, finding the most adequate method to get a complete characterization of the emission implies the selection of the appropriate model, which better explains the processes of generation, propagation and capture of the emitted signals. This description matches the issue of measurement termite activity.

This paper presents the improved equipment over previous prototype's performance, based in the time-frequency domain analysis of the kurtosis, described in [1-2]. The measurement method is based in the interpretation of the spectral kurtosis (SK) graph, along with the wavelet analysis, which is thought as an aid. At the same time, we use a simple data acquisition unit, the sound card (maximum speed at 44.1 kHz), which simplifies the hardware unit and the criterion of detection. The instruments for plague detection are thought with the objective of decreasing subjectivity of the field operator [1-5]. On-site monitoring implies reproducing the natural phenomenon of insect emissions with high accuracy. As a consequence it is imperative the use of a deep storage device, and high sensitive probes with a selective frequency response. These features make the price paid high, and do not guarantee the success of the detection.

Regarding the procedures, the prior detection methods are very much dependent on the detection of the excess of power in the signals; these are the so-called second-order methods. For

example, the RMS calculation can only characterize the intensity, and does not provide information regarding the envelope of the signal nor the amplitude fluctuations. Another handicap of the second-order principle, e.g. the power spectrum, attends to the preservation of the energy during data processing. Consequently, the eradication of additive noise lies in filter design and sub-band decomposition, like wavelets and wavelet packets.

As an alternative to improve noise rejection and complete characterization of the signals, in the past ten years, a myriad of higher-order statistics (HOS) methods are being applied in different fields of science and technology, in scenarios involving signal separation and characterization of non-Gaussian measurements [6]. Concretely, the area of diagnostics-monitoring of rotating machines is also under our interest due to the similarities of the signals to be monitored with the transients from termites. Many time-series of faulty rotating machines consist of more-or-less repetitive short transients of random amplitudes and random occurrences of the impulses [7].

This paper describes a method based in the SK (related to the fourth-order cumulant at zero lags) to detect infestations of subterranean termites in a real-life scenario (southern Spain). Wavelet decomposition is used as an extra tool to aid detection from the preservation of the approximation of the signal, which is thought to be more Gaussian than the details.

The interpretation of the results is focused on the peakedness of the statistical probability distribution associated to each frequency component of the signal, to get a measure of the distance from the Gaussian distribution. The SK serves as a twofold tool. First, it enhances non-Gaussian signals over the background. Secondly, it offers a more complete characterization of the transients emitted by the insects, providing the user with the probability associated to each frequency component.

The paper is structured as follows: in the following section a review on termite detection and relevant HOS experiences sets the foundations. Then we make a brief report on the definition of kurtosis; we use an unbiased estimator of the SK, successfully used in [1-2]. Results are presented thereafter. Finally, conclusions are drawn.

### **Subterranean Termites: Detection project towards HOS**

Termite detection has been gaining importance within the research community in the last two decades, mainly due to the urgency of avoiding the use of harming termiticides, and to the joint use of new emerging techniques of detection and hormonal treatments, with the aim of performing an early treatment of the infestation. A localized partial infestation can be exterminated after two or three generations of the colony's members with the aid of these hormones, which stop chitin synthesis. A chitin synthesis inhibitor kills termites by inhibiting formation of a new exoskeleton when they shed their old one. As a direct consequence, the weakened unprotected workers stop feeding the queen termite, which dies of starvation.

The primary method of termite detection consists of looking for evidence of activity. But only about 25 % of the building structure is accessible, and the conclusions depend very much on the level of expertise and the criteria of the inspector [1-5]. As a consequence, new techniques have been developed to remove subjectivity and gain accessibility.

User-friendly equipment is currently used in targeting subterranean infestations by means of temporal analysis of the vibratory data sequences. An acoustic-emission (AE) sensor or an accelerometer is fixed to the suspicious structure. This class of instruments is based on the calculation of the RMS value of the vibratory waveform. The RMS value comprises information of the AE raw signal power during each time-interval of measurement (averaging time). This measurement strategy conveys a loss of potentially valuable information both in the time and in the frequency domain [1-5]. A more sophisticated family of instruments makes use of spectral analysis and digital filtering to detect and characterize vibratory signals [4]. Other second-order tools, like wavelets and wavelet packets (time-dependent technique) concentrate on transients and non-stationary movements, making possible the detection of singularities and sharp transitions, by means of sub-band decomposition.

Higher-order statistics are being widely used in several fields. The spectral kurtosis has been successfully described and applied to the vibratory surveillance and diagnostics of rotating machines [7]. In the field of insect detection, the work presented in [2] set the foundations of the present paper. The combined use of the SK and the time-domain sliding kurtosis showed marked features associated to termite emissions. In the frequency domain (sample frequency 64.0 kHz), three frequency zones were identified in the spectral kurtosis graph as evidence of infestation; two in the audio band (which will be also checked in the present paper) and one in the near ultrasound (roughly equal to 22 kHz). In the present paper the sample frequency was fixed to 44.1 kHz and the sound card was directly driven by MATLAB. Results are presented in the user interface, which is shown in Fig. 1; in this measurement situation, the time-raw data contains alarms and activity signals from termites. This is a clear example of positive detection.

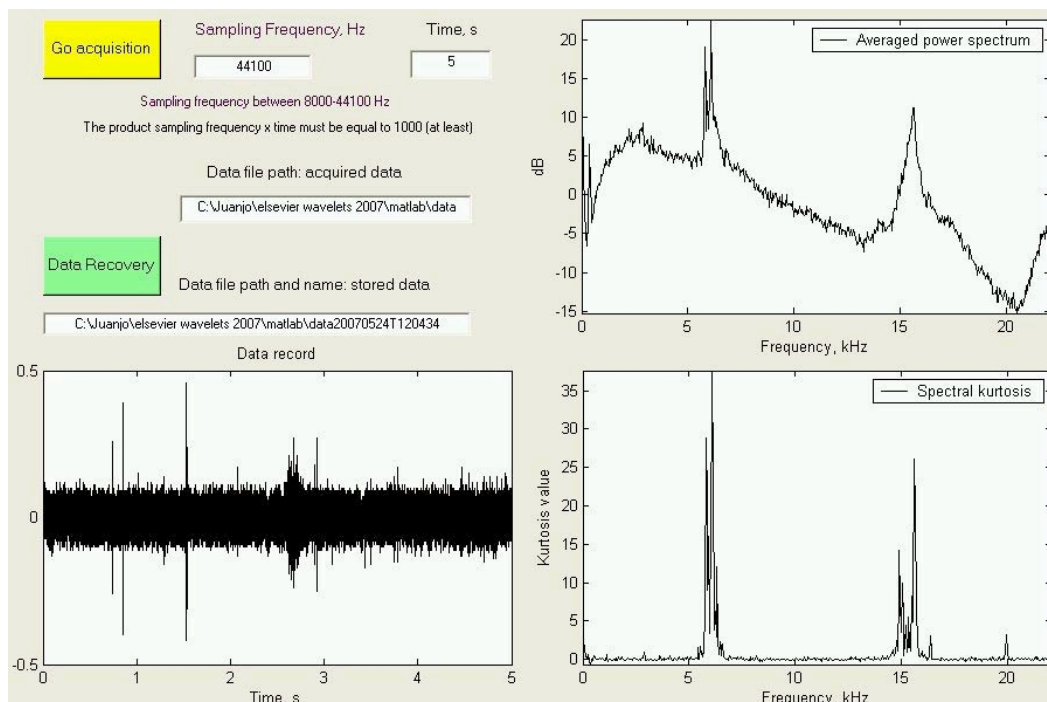


Fig. 1. The graphical user interface, which presents the results to the field operator. The SK graph is in the bottom-right corner.

The developed virtual instrument also calculates and presents the spectrum (upper-right) and the raw data (bottom-left). The field operator adds therefore visual information to the classical audio-based criterion, which was by the way very subjective and very expertise-dependent.

## Kurtosis and the SK Estimator

Kurtosis is a measure of the "peakedness" of the probability distribution of a real-valued random variable. Higher kurtosis means more of the variance is due to infrequent extreme deviations, as opposed to frequent modestly-sized deviations. This fact is used in this paper to detect termite AE in an urban background. Kurtosis is more commonly defined as the fourth central cumulant divided by the square of the variance of the probability distribution, which is the so-called excess kurtosis, i.e. [2, 8-9]:

$$\gamma_{4,x} = E\{x^4(t)\} - 3(\gamma_{2,x})^2 = C_{4,x}(0,0,0) \quad (1)$$

Ideally, the SK is a representation of the kurtosis of each frequency component of a process (or data from a measurement instrument,  $X_i$ ). For estimation issues, we will consider  $M$  realizations of the process; each containing  $N$  points; i.e. we consider  $M$  measurement sweeps, each sweep with  $N$  points. The time spacing between points is the sampling period  $T_s$ .

A biased estimator for the spectral kurtosis and for a number  $M$  of  $N$ -point realizations at the frequency index  $m$ , is given by [2]:

$$\hat{G}_{2,X}^{N,M}(m) = \frac{M}{M-1} \left[ \frac{(M+1) \sum_{i=1}^M |X_N^i(m)|^4}{\left( \sum_{i=1}^M |X_N^i(m)|^2 \right)^2} - 2 \right]. \quad (2)$$

This estimator is the one we have implemented in the program code in order to perform the data computation and it was also used successfully in [2].

Regarding the experimental signals, we expect to detect positive peaks in the kurtosis's spectrum, which may be associated to termite AE, characterized by random-amplitude impulse-like events. This non-Gaussian behavior should be enhanced over the symmetrically distributed electronic noise, introduced in the measurement system. Speech is perhaps also reflected in the SK, but not in the frequencies where termite emissions manifest. Besides, we assume, as a starting point, that non-Gaussian behavior of termite emissions is more acute than in speech. As a consequence, these emissions would be clearly outlined in the kurtosis spectrum. As a final remark, we expect that constant amplitude interferences are clearly differentiated due to their negative peaks in the SK.

To show the ideal performance of the estimator, which has been described in these lines, and also described in [1-2], we show an example based in synthetics. A mixture of six different signals has been designed. Each mixture is the sum of a constant-amplitude sine wave of 2 kHz, a constant-amplitude sine wave at 9 kHz, a Gaussian-distributed-amplitude sine wave at 5 kHz, a Gaussian-distributed-amplitude sine wave at 18 kHz, a Gaussian white noise, and a colored Gaussian noise between 12 and 13 kHz. Each mixture (realization or sample register) contains 1324 points. Negative kurtosis is expected for constant-amplitude processes, positive kurtosis should be associated to random-amplitudes and zero kurtosis will characterize both Gaussian-noise processes.

A simulation has been made in order to show the influence of the number of sample registers ( $M$ ) in the averaged results for the SK graph, and to test its performance. Figure 2 shows a good performance because enough registers have been averaged ( $M=500$ ).

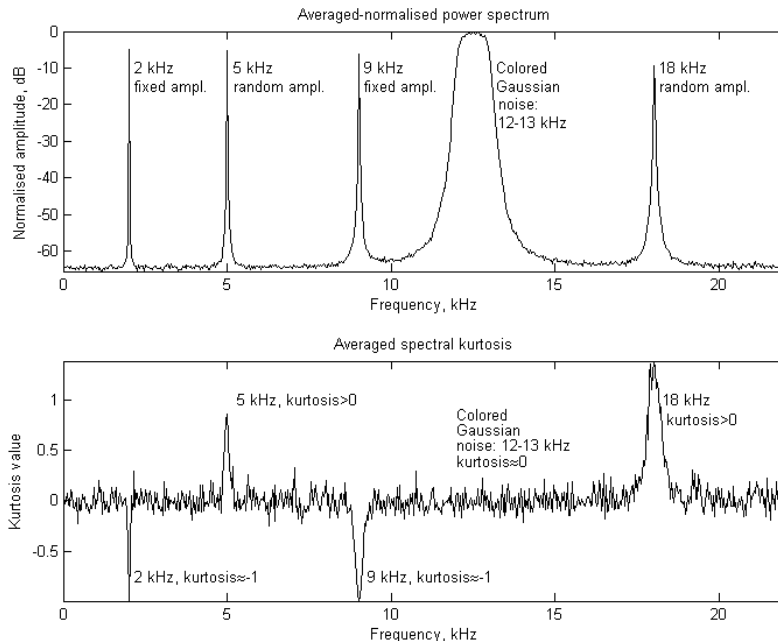


Fig. 2. Performance of the SK estimator over a set, mixed of synthetics.

### De-noising strategy via wavelets. Selecting the optimum decomposition level

The mother wavelet *Daubechies 5* has been selected as the most similar mother wavelet, because of the highest coefficients in the decomposition tree. Given the mother wavelet, to show the process of selecting the maximum decomposition level in the wavelet tree, we have adopted a criterion based on the calculation of *Shannon's* entropy (information entropy), which is a measure of the uncertainty associated with a random variable,  $X$ ; this entropy denoted by  $H(X)$ , and defined by Eq. (3):

$$H(X) = - \sum_{i=1}^N p(x_i) \log_{10} [p(x_i)], \quad (3)$$

where  $X$  is an  $N$ -outcome measurement process  $\{x_i = 1 \dots N\}$ , and  $p(x_i)$  is the probability density function of the outcome  $x_i$ .

We show the strategy via the following example, based on real-life data, like the recordings of Fig. 1, Fig. 4(a) and (b). The entropy of the approximations and the details are compared for each level of comparison as shown in Fig. 3. By looking at the entropy evolution graph of Fig. 3, we see that at level 4, the entropy of the approximations is less than the entropy of the details. So, level 3 is in a sense, a point of entropy inversion. On the other hand, level 4 exhibits the lowest entropy being at the same time lower than the details' entropy. No improvement is obtained for level 5, where these entropies are very similar (approximations and details' entropies are almost the same). We can also see that the global difference of entropies increases towards zero, at level 5, as a complementary indication that further decomposition will not suppose progress in de-noising. This decomposition strategy is satisfied for the 98 % of the data registers, collected at the same place.

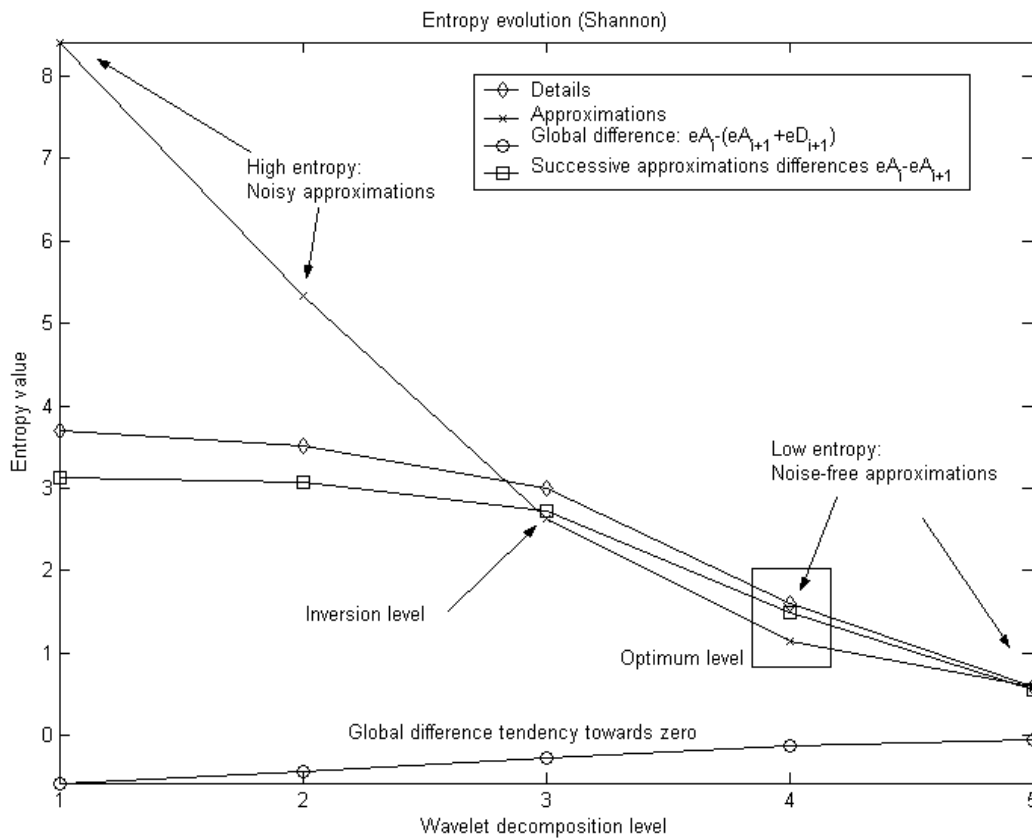


Fig. 3. Entropy evolution showing the optimum level (4). Level 3 is an inversion point and level 4 exhibits the lowest entropy being at the same time lower than the details' entropy.

## Experiment and Results

In this section we describe the experiment and measurement situations. A piezoelectric probe (model SP-1L, Acoustic Emission Consulting) is used in the final version of the instrument, and was described in detail in [2]. The sensor is connected to the sound card of a lap-top computer and the acquisition is driven by MATLAB, via the Graphical User Interface (GUI). The user interface was presented in Fig. 1. The operator can select the acquisition time and the sample frequency (maximum 44.1 kHz). In the bottom-right corner of Fig. 1, the SK graph is presented. The user can also examine the raw data and the spectrum. Automatically, the instrument saves the acquired data (labeling the file with the date). Additionally, the operator can recall the stored files.

The electronic transducer is presented in Fig. 4, along with its charge-to-volt conversion modulus (Integrated Circuit Piezoelectric; ICP interface), and the accessory to fix it in the wood that we used to test the sensor's performance in the lab. A bare waveguide has been used for insertion into soil. With the aim to have a frequency characterization of the sensor we test its impulsive response in the lab by emulating a fiber breaking in a piece of wood, where the sensor was attached via the drill bit. The witness instrument was a high-performance digital storage oscilloscope (Agilent-54622A). In Fig. 5, we show a photo of the calibration session, where the instrument's display shows a single capture (and its associated power spectrum) of the vibratory and AE signal once it has propagated through the wood. We can appreciate two differentiated frequency bands. The first 30 kHz resonant band offer the possibility of sensing AE signals from

termites (feeding and excavating). Then we find a resonant bump around 100 kHz (only for the sensor SP1-H), which by the way has been useful for ultrasonic purposes by the research team.

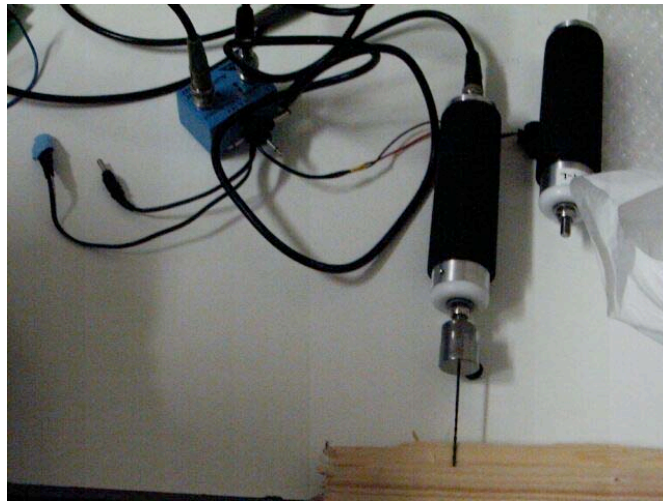


Fig. 4. A photograph of the sensors SP1-L and SP1-H, with the mounted accessories (drill bit) prepared to couple it into the a test-piece of wood, in our lab. On the left, the charge-to-volt converter according to the Integrated Circuit Piezoelectric (ICP) protocol.

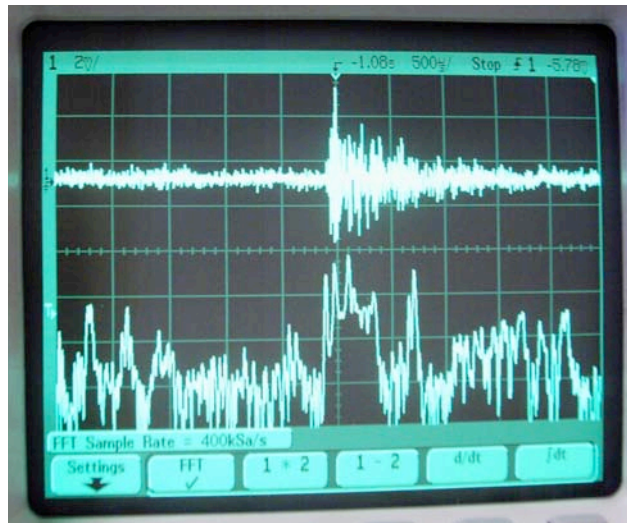


Fig. 5. A photograph of the testing lab session with the sensor SP1-H (a high frequency version of the SP1-L) and a deep memory digital-storage oscilloscope. The acoustic emission event has been sampled at 400 kHz. Horizontal division = 20 kHz.

Termite sounds from feeding are like sharp pops and crackles in the audio output [1-2]. Hit rates of 25-100 /s are common in infestation. The key of the SK detection strategy used in this work lies in the potential enhancement of the non-Gaussian behavior of these emissions. If this happens, i.e. if an increase of the non-Gaussian activity (increase in the kurtosis, peakedness of the probability distribution) is observed in the SK graph, there may be infestation in the surrounding subterranean perimeter, where the transducer is attached.

An additional remark (justifying the use of the SK graph) lies in the fact that the kurtosis as a global indicator, considered as the average of the kurtosis computed for each individual frequency component, is not a valid tool to target termite activity. This is due to the fact that no

discrimination is made among the frequency bands of the emissions, which may be originated by different agents.

Hereinafter, in addition to the detection measurement situation presented in Fig. 1, where the detection is clear, other situations are outlined. In Fig. 6(a) a doubtful measurement case is presented. Activity evidence (low-level alarms) is outlined only near 6 kHz. Once, the wavelets have been applied, shown in Fig. 6(b), the enhancement near 6 kHz and 16 kHz confirms the detection.

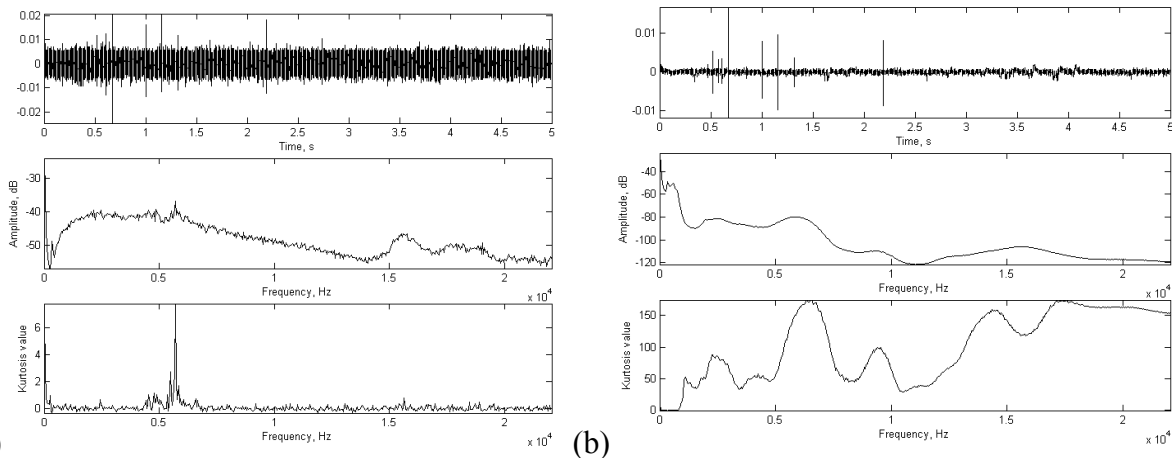


Fig. 6. (a) A doubtful measurement situation without de-noising, where probably low-level alarm signals predominate. (b) De-noising confirms activity, eliciting the bump near 6 kHz and the enhanced zone near 16 kHz.

The next figures, Fig. 7 (a) and (b), show the measurement's performance over a background. In the time-domain, the impulses that are similar to Dirac's deltas are associated to cracks or little movements of the sensor while attached in the ground. So it is important to distinguish these false positives from the impulses induced by termites. De-noising neither add new information nor reveal termite infestation. The impulses in the time domain are the classical artificial cracks resulting for the movement of the sensor in the soil.

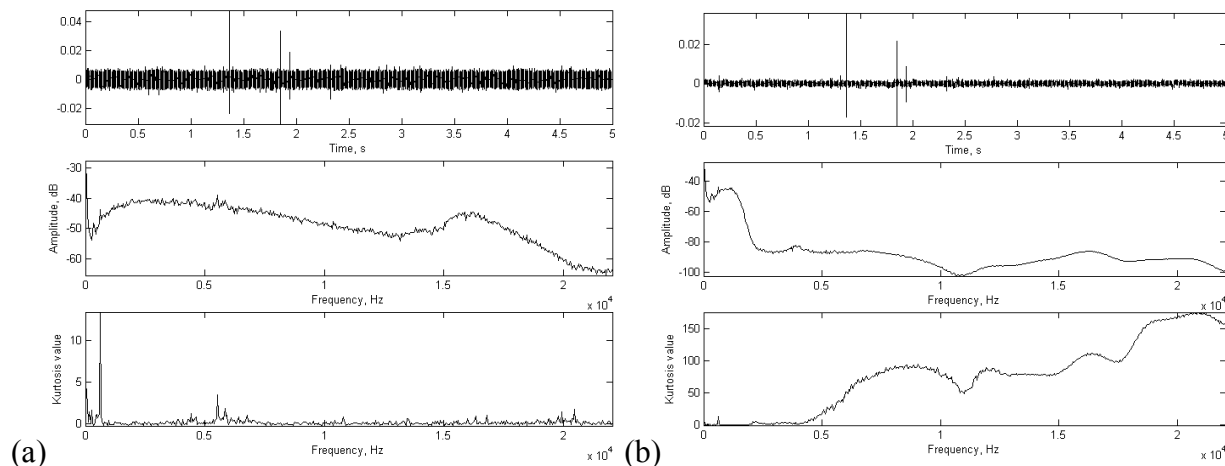


Fig. 7. (a) SK calculation over a background sample register. No activity is seen in the surroundings of the characteristic frequencies. (b) De-noising does not reveal infestation.



The final figures, Fig. 8 (a) and (b), represent another case of detection. This time detection is very clear and again, we can observe the clear bumps near the characteristic frequencies. The bump at the left of 6 kHz reflects the presence of alarms but probably far from the termites whose activity produces the bumps at the right of 6 kHz and 16 kHz. The spectral kurtosis of the de-noised register exhibits several frequency bumps, not only for the frequencies in the interest zones (6 kHz and 16 kHz), but also for the rest of the audio signals. These figures have shown that, despite the fact that audio signals can exhibit non-Gaussian behavior, the non-Gaussian degree of termite activity is higher.

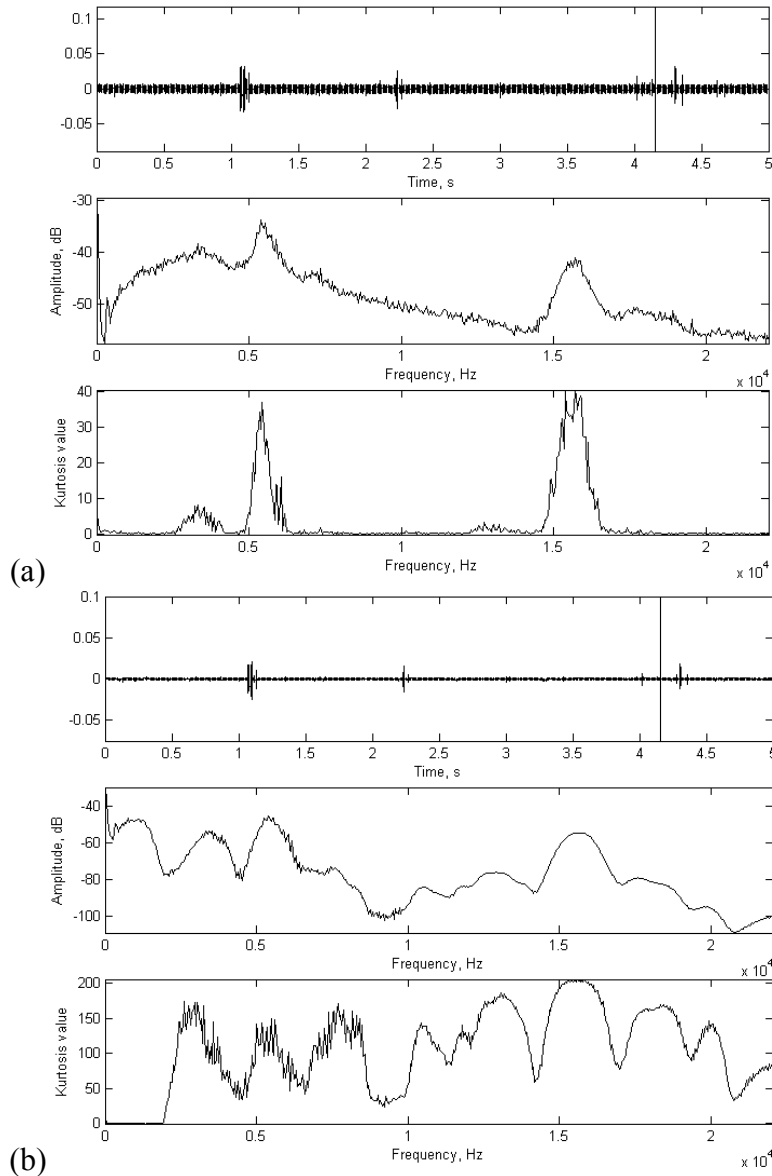


Fig. 8. (a) A clear targeting case with a higher degree of activity. (b) De-noising confirms infestation.

## Conclusion

Assuming the starting hypothesis that the insect emissions may have a more peaked probability distribution than any other simultaneous source of emission in the measurement perimeter, we have design a termite detection strategy and a virtual instrument based in the calculation of the 4th-order cumulants for zero time lags, which are indicative of the signals'

kurtosis. The instrument is actually in use by a Spanish company. An estimator of the spectral kurtosis has been used to perform a selective analysis of the peakedness of the signal. It has been shown that new frequency components gain in relevance in the spectral SK graphs. The main goal of this signal-processing method is to reduce subjectivity due to visual or listening inspection of the registers. This means that in a noisy environment, it may be possible to ignore termite feeding activity even with an *ad hoc* sensor because, despite the fact that the sensor is capable of registering these low-level emissions, the human ear can easily ignore them [2]. The SK signal processing modulus complements human's ear, adding higher-order statistical features, which improve detection, thanks to the noise rejection action, enhancing non-Gaussian features.

## Acknowledgments

The authors would like to thank the Spanish Ministry of Science and Education for funding the PETRI project PTR95-0824-OP dealing with plague detection using higher-order statistics. Our unforgettable thanks to the trust we have from the Andalusian Government for funding the excellence project PAI2005-TIC00155.

## References

1. De la Rosa, J. J. G., Gallego, A., Piotrkowski, R., Castro, E. and Moreno, A. (2008). Spectral kurtosis-based virtual instrument for non-destructive acoustic emission targeting of termites. Proceedings of The 28-th European Conference on Acoustic Emission Testing, September 17-19, Kraków, Poland, pp. 94-99.
2. De la Rosa, J. J. G. and Muñoz, A. M. (2008). Higher-order cumulants and spectral kurtosis for early detection of subterranean termites. *Mechanical Systems and Signal Processing (Ed. Elsevier)*, **22** (1): 279–294. Available online 1 September 2007.
3. De la Rosa, J. J. G., Lloret, I., Moreno, A., Puntonet, C. G., and Górriz, J. M. (2006). Wavelets and wavelet packets applied to detect and characterize transient alarm signals from termites. *Measurement (Ed. Elsevier)*, **39**(6): 553–564. Available online 10 January 2006.
4. Mankin, R. W. and Fisher, J. R. (2002). Current and potential uses of acoustic systems for detection of soil insects infestations. In *Proceedings of the Fourth Symposium on Agroacoustic*, pages 152–158.
5. Robbins, W. P., Mueller, R. K., Schaal, T., and Ebeling, T. (1991). Characteristics of acoustic emission signals generated by termite activity in wood. In *Proceedings of the IEEE Ultrasonic Symposium*, pages 1047–1051.
6. De la Rosa, J. J. G., Piotrkowski, R., and Ruzzante, J. (2007b). Third-order spectral characterization of acoustic emission signals in ring-type samples from steel pipes for the oil industry. *Mechanical Systems and Signal Processing (Ed. Elsevier)*, **21**(4): 1917–1926. Available online 10 October 2006.
7. Antoni, J. (2006b). The spectral kurtosis: application to the vibratory surveillance and diagnostics of rotating machines. *Mechanical Systems and Signal Processing (Ed. Elsevier)*, **20**(2): 308–331.
8. Mendel, J. M. (1991). Tutorial on higher-order statistics (spectra) in signal processing and system theory: Theoretical results and some applications. *Proceedings of the IEEE*, **79**(3): 278–305.
9. Nikias, C. L. and Mendel, J. M. (1993). Signal processing with higher-order spectra. *IEEE Signal Processing Magazine*, pages 10–37.